Asian Journal of Chemistry; Vol. 38, No. 9 (2026), 2301-2313
ASIAN JOURNAL OF CHEMISTRY
https://doi.org/10.14233/ajchem.2026.36449

Synthesis, Antioxidant, Analgesic, Anti-Inflammatory Activities and Molecular Docking Studies of Newly 1,2,4-Triazole-3-yl-sulfanyl-acetamide Derivatives

SANTANU KUMAR HOTTA[1,*], SUDHANSHU SEKHAR ROUT[1], ANJAN KUMAR[2], GHANSHYAM PANIGRAHI[3] and P. CHIRANJEEVI[4]

[1]School of Pharmaceutical Sciences, Siksha 'O' Anusandhan Deemed to be University, Bhubaneswar-751003, India
[2]Department of Pharmaceutical Chemistry, Roland Institute of Pharmaceutical Sciences, Berhampur-760010, India
[3]Department of Pharmacology, Royal College of Pharmacy and Health Sciences, Berhampur-760002, India
[4]Department of Pharmaceutical Chemistry, Vignan Institute of Pharmaceutical Technology, Visakhapatnam-530049, India

*Corresponding author: E-mail: shaanhotta@gmail.com

Received: 17 May 2026 *Accepted*: 14 July 2026 *Published online*: 5 September 2026 AJC-22458

A series of ten 1,2,4-triazole-3-yl-sulfanyl-acetamide derivatives bearing a mercapto (-SH) group were synthesized and characterized using FTIR, ^{1}H NMR, ^{13}C NMR, UV, mass spectrometry and DSC. The compounds were prepared within two structural frameworks: (i) N-(*p*-toluoyl)-{[4-phenyl-5-(pyridin-4-yl)-4*H*-1,2,4-triazol-3-yl]sulfanyl}acetamide and (ii) N-[4-(1-oxo-3-phenyl-propenyl)phenyl]-2-(4-phenyl-5-pyridin-4-yl-4*H*-1,2,4-triazol-3-ylsulfanyl)acetamide. Molecular docking against COX-2 (PDB ID: 5F1A) highlighted compound **4a** from framework I (binding energy -12.09 kcal mol^{-1}) and compound **5e** from framework II (binding energy -13.15 kcal mol^{-1}) as the most promising compounds with favourable interactions, supporting their potential as lead molecules for further biological evaluation. In addition, physico-chemical, pharmacokinetic and HOMO-LUMO (ΔE_{H-L} = 9.985 and 9.986 eV) also suggested that **4a** and **5e** are two lead candidates with positive drug-ability profiles (0.60 and 0.68). Prior to selecting safe/non-toxic doses of both leads for biological activity, the acute oral toxicity was investigated following the OECD-423 guidelines, where 200 and 400 mg/kg were selected as non-toxic doses for *in vivo* biological activity. The analgesic activity of the lead compounds **4a** and **5e** was evaluated in Wistar albino rats using the Eddy's hot plate method. Anti-inflammatory effects were investigated through both *in vitro* protein denaturation assays (employing hot and cold-water extracts) and the *in vivo* carrageenan-induced paw edema model. The antioxidant potential of **4a** and **5e** was evaluated using the DPPH radical scavenging assay. Structural variation from the simple aryl scaffold of **4a** to the chalcone framework of **5e** provided insight into the structure–activity relationship. The *ortho*-hydroxy substituent in **5e** enhanced radical-scavenging capacity and may contribute to its activity against oxidative stress, pain and inflammation. *In silico*, *in vitro* and *in vivo* findings identified **4a** and **5e** as promising derivatives with favourable analgesic, anti-inflammatory, antioxidant and drug-likeness profiles.

Keywords: 1,2,4-Triazole-3-yl-sulfanylacetamides, Biological activities, Molecular docking, ADMET prediction.

INTRODUCTION

Drug discovery involves a complex progression from scaffold identification to clinical validation, requiring extensive biological, pharmacokinetic and safety assessments with a low probability of clinical success [1-3]. The growing burden of antimicrobial resistance, inflammation and oxidative stress related disorders creates a need for safer and more effective therapeutic scaffolds [4-7]. Medicinal chemistry approaches such as scaffold modification, isosteric replacement and pharmacophore hybridization facilitate the design of bioactive molecules, while advanced formulation strategies can improve solubility, bioavailability and target delivery [8-14].

Heterocyclic scaffolds remain central to drug discovery due to their structural diversity and broad pharmacological potential [15-19]. Among these, 1,2,4-triazole possesses favourable physico-chemical characteristics, high stability and versatile biological activity [20-23]. Its nitrogen-rich ring can establish interactions with enzymes and receptors involved in inflammation, nociception and oxidative stress [24-26]. 1,2,4-Triazole derivatives have been investigated as COX modulators, antioxidant agents and analgesic candidates, providing a useful framework for developing multifunctional therapeutic molecules [27-30].

Sulfur-containing heterocycles are important scaffolds in drug discovery, with sulfur incorporation often influencing

lipophilicity, bioavailability and target interactions [31-33]. Mercapto (–SH) and imine (–C=NH) functionalities contribute to antioxidant, analgesic and anti-inflammatory properties through electron donation, radical stabilization and interactions with biological targets [34-37]. Their integration with 1,2,4-triazole offers a rational basis for developing multifunctional 1,2,4-triazole-3-yl-sulfanyl-acetamide derivatives.

Based on this rationale, two series of derivatives were designed and synthesized, followed by spectroscopic characterization and *in vitro*, *in vivo* and *in silico* evaluation. Antioxidant, analgesic, anti-inflammatory and acute oral toxicity profiles were investigated using complementary experimental models. Molecular docking against COX-2, ADMET analysis and HOMO–LUMO calculations were employed to examine target interactions, pharmacokinetic characteristics and electronic properties [38,39]. COX-2 was selected due of its established role in inflammation, pain and oxidative-stress associated signalling. Radical-scavenging assays were performed separately to assess the intrinsic antioxidant capacity of the synthesized compounds and their potential as multifunctional therapeutic leads.

EXPERIMENTAL

The synthetic-grade chemicals and reagents were purchased from Loba Chemie Pvt. Ltd, India. The completion of the reaction was determined by thin-layer chromatography (TLC) with a single spot on precoated silica gel G60 F_{254} plates (0.2 mm, Merck) using the solvent system toluene:acetone (8:2). The functional moieties that confirm the structure of the synthesized products were analyzed with KBr discs on the Shimadzu FTIR-8400 spectrophotometer. The environments of the structural skeleton were analyzed with proton nuclear magnetic resonance (^{1}H NMR) and ^{13}C NMR spectra using a Bruker DPX-400 MHz spectrometer. Mass spectral data were recorded on a Shimadzu mass spectrometer and differential scanning calorimetry (DSC) was also performed for thermal analysis. The melting points of the synthesized compounds were measured using open capillaries and an electrothermal device.

Synthesis: Following the previous protocol, a total of ten derivatives of 1,2,4-triazole-3-yl-sulfanyl-acetamide were synthesized [40,41]. Initially, the mixture of 4-phenyl-5-(pyridine-4-yl)-4*H*-1,2,4-triazole-3-thiol (0.01 mol) and 2-chloro-*N*-(aryl)-acetamide (0.01 mol) in 50 mL dry acetone and anhydrous K_2CO_3 (0.02 mol) was stirred for 4 h at room temperature and poured into ice; the product was filtered and washed with cold water (**Scheme-I**). Similarly, the mixture of 4-phenyl-5-(pyridine-4-yl)-4*H*-1,2,4-triazole-3-thiol (0.01 mol) and 2-1-(4-acetylphenyl)amino)-*N*-chloroacetamide (0.01 mol) in 50 mL dry acetone and anhydrous K_2CO_3 (0.02 mol) was stirred for few hours at room temperature and poured into ice; the product was filtered and washed with cold water (**Scheme-II**).

2-((4-Phenyl-5-(pyridin-4-yl)-4*H*-1,2,4-triazol-3-yl)thio)-*N*-(*p*-tolyl)acetamide (4a): Yield: 1.49 g (82%); garnet-red solid; m.p.: 164-172 ºC; R_f: 0.61; UV-Visible (λ_{max}, toluene: acetone): 291 nm; Elemental analysis of $C_{22}H_{19}N_5SO$; calcd. (found) %: C, 68.02 (65.82); H, 4.93 (4.77); N, 17.99 (17.44); O, 4.12 (3.98); S, 9.94 (9.99); FTIR (KBr, ν_{max}, cm^{-1}): 3065 (C-H *str*. arom.), 3310 (-NH *str*. 2º NH_2), 2918 (C-H *str*.), 1681 (-C=O *str*.), 1614 (-S-C=O *str*. in thioester linkage), 1600 (-C=N *str*.), 1512 (-C=N *str*.), 1430 (-C=C- *str*.); ^{1}H NMR (400 MHz, DMSO-d_6, δ ppm): 8.76 (d, 2H) pyridine (Ar-H); 7.49-7.32 (m, 5H) (Ar-H), 7.30-7.28 (d, 2H) (Ar-H), 7.19 (d, 2H) (Ar-H), 7.13-7.04 (d, 2H), 4.13 (s, 2H) (s, 3H) (Ar-CH_3); ^{13}C NMR (125 MHz, DMSO-d_6, δ ppm): 162.4, 150.7, 150.2, 150.0, 149.7, 141.2, 134.6, 130.8, 129.5, 129.3, 127.7, 123.7, 123.6, 121.1, 121.6; mass spectra (*m/z*) $[M^+H]^+$: 402.6.

***N*-(4-Methoxyphenyl)-2-((4-phenyl-5-(pyridin-4-yl)-4*H*-1,2,4-triazol-3-yl)thio)-acetamide (4b):** Yield: 1.41 g (78.2%); white solid; m.p.: 160 ºC; R_f: 0.64; Elemental analysis of $C_{22}H_{19}N_5SO_2$; calcd. (found) %: C, 65.45 (63.29); H, 4.75 (4.59); N, 17.85 (16.78); O, 7.94 (7.66); S, 7.95 (7.68); FTIR (KBr, ν_{max}, cm^{-1}): 3383 (-NH *str*. in amide); 1636 (C=O in amide), 1610 (S-C=O in thioester linkage); 1518 (C=N), 1445 (C=C arom.); ^{1}H NMR (400 MHz, DMSO-d_6, δ ppm): 3.60 (s, 3H, OCH), 4.26 (s, 2H, CH_2), 7.09-7.11 (d, *J* = 8, 2H, Ar-H), 7.21-7.23 (d, *J* = 4 Hz, 2H, Ar-H), 7.41-7.48 (m, 5H, Ar-H), 7.51-7.53 (d, *J* = 8 Hz, 1H, Ar-H), 8.52-8.54 (d, *J* = 8, 2H, Ar-H), 10.25 (s, 1H, -NH); mass spectra (*m/z*):418.7 (M^+).

***N*-(4-Fluorophenyl)-2-{[4-phenyl-5-(pyridin-4-yl)-4*H*-1,2,4-triazol-3-yl]sulfanyl}acetamide (4c):** Yield: 1.39 g (70.4%); yellow solid; m.p.: 158 ºC; R_f: 0.53; Elemental analysis of $C_{21}H_{16}N_5SOF$; Calcd. %: C, 63.63 (62.21); H, 4.07 (3.98); N, 17.67 (17.27); O, 4.04 (3.95); S, 8.10 (7.91); F, 4.79 (4.69); FTIR (KBr, ν_{max}, cm^{-1}): 3346 (-NH *str*. in amide), 1642 (S-C=O in thioester linkage), 1629 (C=O in amide), 1511 (C=N), 1450 (C=C arom.); ^{1}H NMR (400 MHz, DMSO-d_6, δ ppm): 4.12 (s, 2H, CH_2), 7.13-7.16 (d, *J* = 8 Hz, 2H, Ar-H), 7.24-7.25 (d, *J* = 4 Hz, 2H, Ar-H), 7.44-7.56 (m, 5H, Ar-H), 7.57-7.59 (d, *J* = 8 Hz, 2H, Ar-H), 8.54-8.55 (d, *J* = 8 Hz, 2H, Ar-H), 10.22 (s, 1H, -NH); mass spectra (*m/z*): 427.6 (M^+).

***N*-(4-Nitrophenyl)-2-{[4-phenyl-5-(pyridin-4-yl)-4*H*-1,2,4-triazol-3-yl]sulfanyl}acetamide (4d):** Yield: 1.2 g (64.1%); yellow solid; m.p.: 89 ºC; R_f: 0.58; Elemental analysis of $C_{21}H_{16}N_6O_3S$; calcd. (found) %: C, 58.32 (58.36); H, 3.73 (3.70); N, 19.43 (19.42); O, 11.10 (11.15); S, 7.41 (7.39); FTIR (KBr, ν_{max}, cm^{-1}): 3456 (-NH *str*. in amide), 1668 (C=O in amide), 1633 (S-C=O in thioester linkage), 1544 (C=N), 1454 (C=C arom.); ^{1}H NMR (400 MHz, DMSO-d_6, δ ppm): 4.20 (s, 2H, CH_2), 7.16-7.17 (d, *J* = 8 Hz, 2H, Ar-H), 7.23-7.25 (d, *J* = 4 Hz, 2H, Ar-H), 7.41-7.46 (m, 5H, Ar-H), 7.53-7.55 (d, *J* = 8 Hz, 2H, Ar-H), 8.57-8.59 (d, *J* = 8 Hz, 2H, Ar-H), 10.22 (s, 1H, -NH); mass spectra (*m/z*):433.4 (M^+).

***N*-(3-Bromophenyl)-2-{[4-phenyl-5-(pyridin-4-yl)-4*H*-1,2,4-triazol-3-yl]thio}acetamide (4e):** Yield: 1.7 g (68.5%); yellow solid; m.p.: 162 º C; R_f: 0.67; Elemental analysis of $C_{21}H_{16}N_5SOBr$; calcd. (found) %: C, 54.08 (54.09); H, 3.46 (3.44); N, 15.02 (15.44); O, 3.43 (3.45), S, 6.87 (6.85); Br, 17.14 (17.13); FTIR (KBr, ν_{max}, cm^{-1}): 3368 (-NH *str*. amide), 1654 (C=O in amide), 1640 (S-C=O in thioester linkage), 1544 (C=N), 1421 (C=C arom.); ^{1}H NMR (400 MHz, DMSO-d_6, δ ppm): 4.27 (s, 2H, CH_2), 7.26-7.29 (d, *J* = 4, 2H, Ar-H), 7.54-7.67 (d, *J* = 8 Hz, 2H, Ar-H), 8.53-8.56 (d, *J* = 8 Hz, 2H, Ar-H), 7.17-7.19 (d, *J* = 8 Hz, 2H, Ar-H), 7.43-7.59 (m, 5H, Ar-H), 10.27 (s, 1H, -NH); mass spectra (*m/z*): 467.7 (M^+).

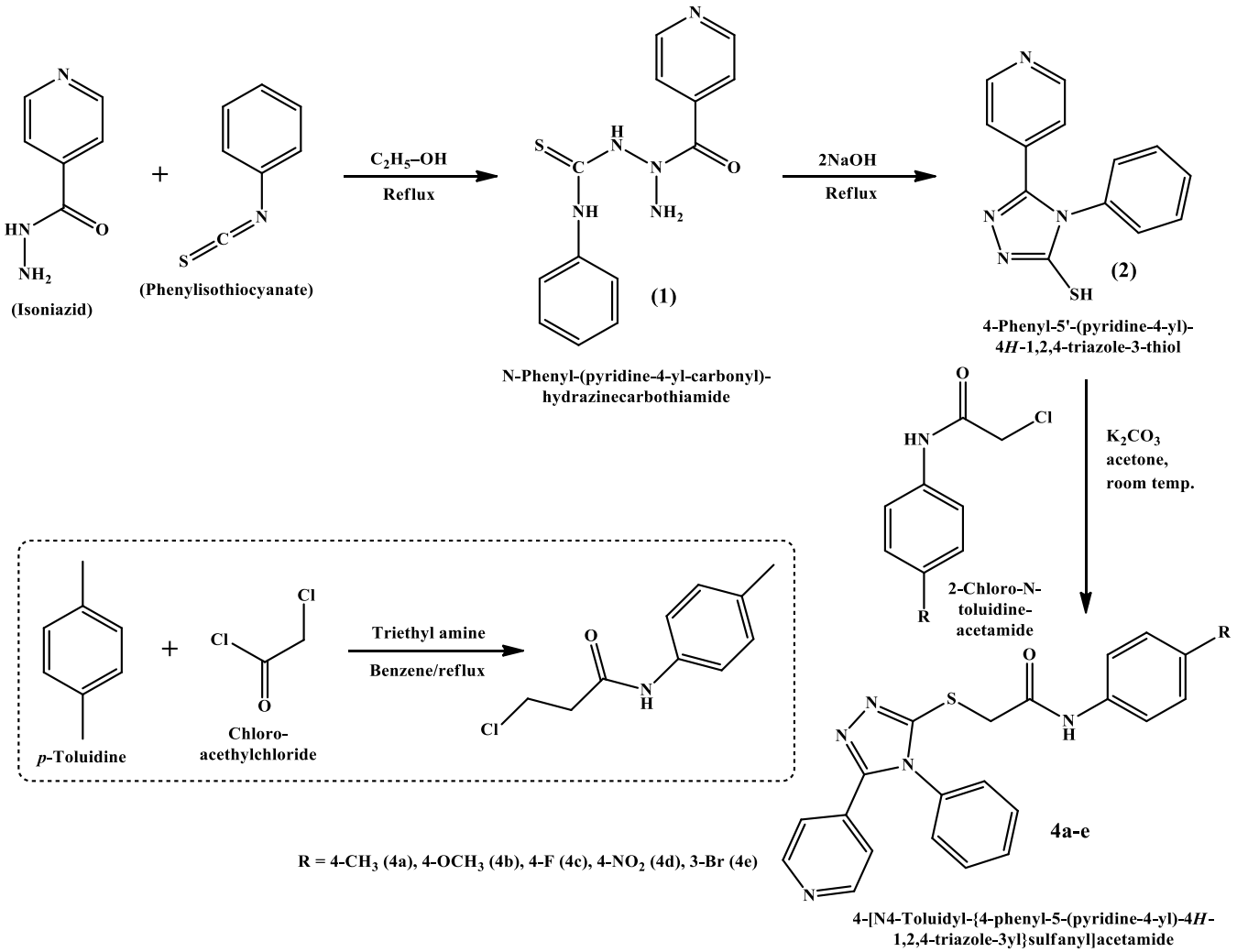

Scheme-I: Synthetic route for 1,2,4-triazole-3yl-sulfanyl-acetamide derivatives (**4a-e**)

(*Z*)-2-(([4-Phenyl-5-pyridine-4yl)-4*H*-[1,2,4]-triazol-3-yl)thio)-*N*-(3-phenylacryloyl)acetamide (5a): Yield: 2 g (71%); white solid; m.p.: 210 º C; R_f: 0.75; Elemental analysis of $C_{30}H_{25}N_5SO_2$; calcd. (found) %: C, 68.17 (69.61); H, 4.77 (4.78); N, 13.25 (13.53); O, 6.06 (.19); S, 7.75 (7.99); IR (KBr, ν_{max}, cm^{-1}): 3414 (-NH_2 *str*.), 3056 (C-H *str*.), 2918 (C-H *str*.), 1665 (-C=O *str*.), 1600 (-C=C/C=N *str*.), 1599 (-S-C=O in thioester linkage), 1540 (-C=N *str*.), 1430 (-C=C- *str*.); ^{1}H NMR (400 MHz, DMSO-d_6, δ ppm): 7.099-7.402 (s, 1H, Ar-H), 7.404-7.504 (d, 1H) (Ar-H), 7.482-7.521 (s, 1H, -CH=CH_2), 8.149 (m, 7H, Ar-H), 8.263 (m, 6H, Ar-H), 8.298-8.317 (s, 1H, Ar-H), 8.545-8.968 (s, 1H, Ar-CH_2), 8.981 (s, 1H, Ar-NH); *m/z* (%): 402.6 (M^+).

(*Z*)-*N*-(4-(3-(4-Hydroxyphenyl)acryloyl)phenyl)-2-((4-phenyl-5-pyridin-4-yl)-4*H*-[1,2,4]-triazole-3-yl-thio)-acetamide (5b): Yield: 2.4 g (78%); yellow solid; m.p.: 212 ºC; R_f: 0.57; Elemental analysis of $C_{30}H_{26}N_5SO_3$; calcd. (found) %: C, 67.11 (67.53); H, 4.87 (4.34); N, 13.05 (13.12); O, 8.95 (8.99), S, 5.97 (6.01); IR (KBr, ν_{max}, cm^{-1}): 3411 (-NH_2 *str*.), 3053 (-CH *str*.), 1664 (-C=O *str*.), 2917 (-S-C=O in thioester), 1611 (-C=C-), 1598 (-CH *str*.), 1541 (-C=N *str*.), 1431 (-C=C- *str*.); ^{1}H NMR (400 MHz, DMSO-d_6, δ ppm): 4.34 (s, 2H, Ar-CH_2), 7.29-7.31 (m, 1H, Ar-H), 7.46-7.47 (d, m, Ar-H), 7.49-7.50 (d, 1H, -CH=CH-), 7.51-7.52 (d, 1H, Ar-H), 7.60-7.62 (d, 1H, Ar-H), 7.93-7.94 (d, 1H, Ar-H), 8.56-8.59 (d, 1H, Ar-H), 10.67 (s, 1H, Ar-NH); *m/z* (%): 335 (M^+, 100), 228 (6.7).

(*Z*)-*N*-(4-(3-(3-Nitrophenyl)acryloyl)phenyl)-2-((4-phenyl-5-pyridin-4-yl)-4*H*-[1,2,4]-triazole-3-yl-thio)-acetamide (5c): Yield: 2.1 g (72%); brick red solid; m.p.: 185 º C; R_f: 0.53; Elemental analysis of $C_{30}H_{22}N_6O_4S$; calcd. (found) %: C, 64.00 (64.05); H, 3.94 (3.94); N, 14.94 (14.94); O, 11.38 (11.37), S, 5.74 (5.70); IR (KBr, ν_{max}, cm^{-1}): 3413 (-NH_2), 3053 (-CH *str*.), 2917, -CH *str*.), 1664 (-C=O *str*.), 1611 (-C=C- *str*.), 1598 (-S-C=O in thioester), 1541 (-C=N *str*.), 1431 (-C=C- *str*.); ^{1}H NMR (400 MHz, DMSO-d_6, δ ppm): 4.31 (s, 2H, Ar-CH_2), 7.29-7.30 (m, 1H, Ar-H), 7.45-7.47 (d, m, Ar-H), 7.49-7.52 (d, 1H, Ar-H), 7.53-7.54 (d, 1H, -CH=CH-), 7.61-7.62 (d, 1H, Ar-H), 7.95-7.92 (d, 1H, Ar-H), 8.57-8.58 (d, 1H, Ar-H), 10.74 (s, 1H, Ar-NH); *m/z* (%): 335 (M^+, 100), 228 (6.7).

(*Z*)-*N*-(4-(3-(4-Chlorophenyl)acryloyl)phenyl)-2-((4-phenyl-5-pyridin-4-yl)-4*H*-[1,2,4]-triazole-3-yl-thio)-acetamide (5d): Yield: 1.9 g (70%); yellow, solid; m.p.: 184 ºC; R_f: 0.51; Elemental analysis of $C_{30}H_{22}N_5SO_2Cl$; calcd. (found) %: C, 64.46 (65.27); H, 3.97 (4.02); N, 12.52 (12.69);

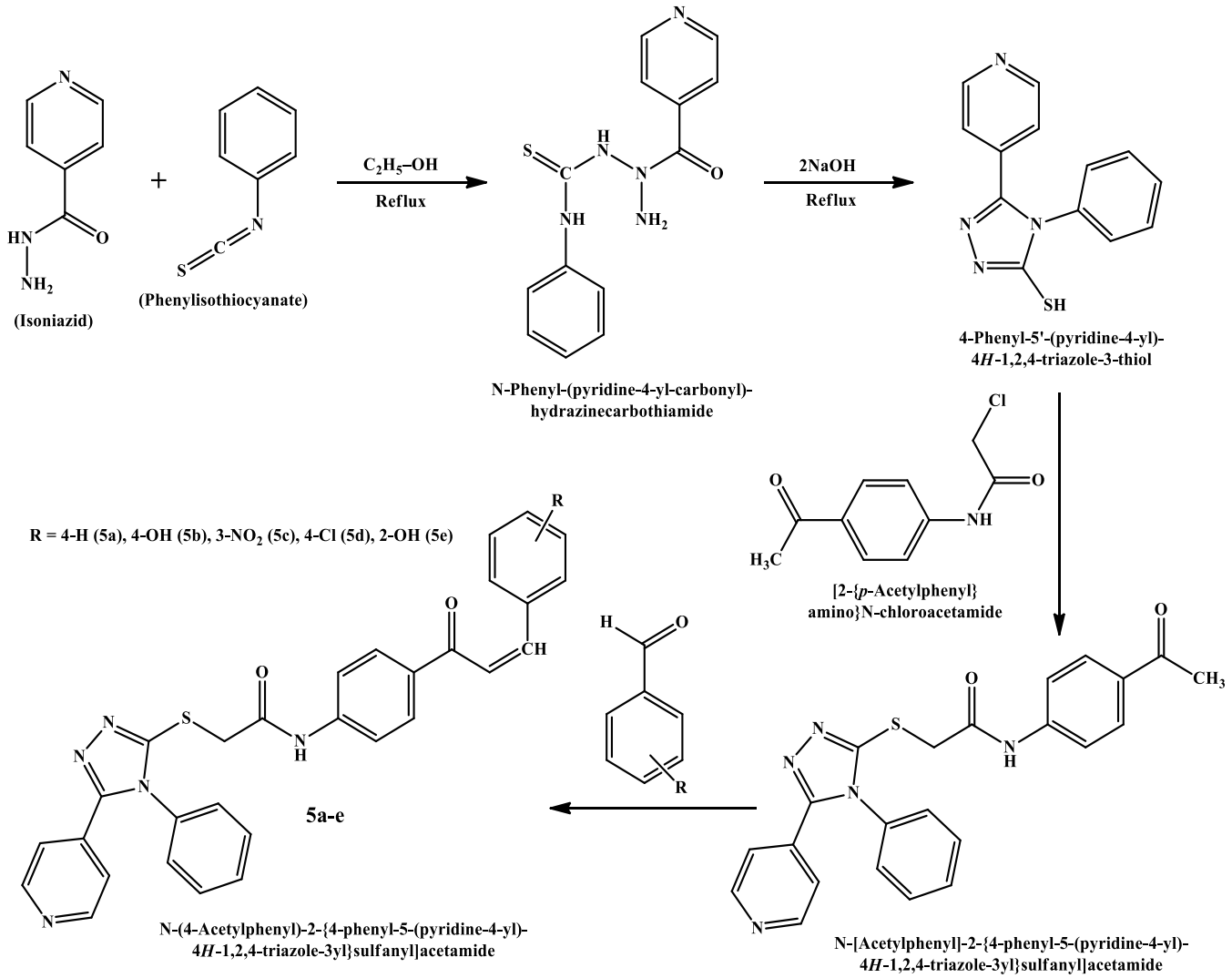

Scheme-II: Synthetic route for 1,2,4-triazole-3yl-sulfanyl-acetamide derivatives (**5a-e**)

O, 5.73 (5.80); S, 5.73 (5.81); Cl, 7.59 (6.42); IR (KBr, ν_{max}, cm^{-1}): 3413 (-NH_2 *str*.), 3053 (-CH *str*.), 1664 (-C=O *str*.), 1611 (-C=C-), 1598 (-S-C=O in thioether), 1541 (-C=N *str*.), 1431 (-C=C-*str*.); ^{1}H NMR (400 MHz, DMSO-d_6, δ ppm): 4.31 (s, 2H, Ar-CH_2), 7.14-7.43 (d, 1C, Ar-H), 7.29-7.30 (m, 1H, Ar-H), 7.45-7.47 (d, m, Ar-H), 7.49-7.52 (d, 1H, Ar-H), 7.61-7.62 (d, 1H, Ar-H), 7.92-7.95 (d, 1H, Ar-H), 10.73 (S, 1H, Ar-NH); *m/z* (%): 335 (M^+, 100), 228 (6.7).

(*Z*)-*N*-(4-(3-(2-Hydroxyphenyl)acryloyl)penyl)-2-((4-phenyl-5-pyridin-4-yl)-4*H*-[1,2,4]-triazole-3-yl-thio)-acetamide (5e): Yield: 2.1 g (73%); white solid; m.p.: 188 ºC; R_f: 0.48; Elemental analysis of $C_{30}H_{23}N_5SO_3$; calcd. (found) %: C, 67.52 (67.53); H, 4.34 (4.36); N, 13.12 (13.10); O, 9.00 (8.99), S, 6.01 (6.05); IR (KBr, ν_{max}, cm^{-1}): 3412 (-NH_2), 3053 (-CH *str*.), 2919 (-CH *str*.), 1664 (-C=O *str*.), 1611 (-C=N-), 1598 (-S-C=O in thioether), 1541 (-C=N *str*.), 1431 (-C=C-*str*.); ^{1}H NMR (400 MHz, DMSO-d_6, δ ppm): 4.33 (s, 2H, Ar-CH_2), 7.28-7.31 (m, 1H, Ar-H), 7.44-7.46 (d, m, Ar-H), 7.49-7.50 (d, 1H, -CH=CH-), 7.53-7.51 (d, 1H, Ar-H), 7.59-7.61 (d, 1H, Ar-H), 7.93-7.94 (d, 1H, Ar-H), 8.54-8.59 (d, 1H, Ar-H), 10.69 (s, 1H, Ar-NH); ^{13}C NMR (400 MHz, DMSO-d_6, δ ppm): 160.53, 158.00, 149.86, 149.66, 144.42, 132.39, 129.41, 40.57, 40.10, 39.95, 39.32; *m/z* (%): 335 (M^+, 100), 228 (6.7).

Acute oral toxicity and analgesic potency investigation: For *in vivo* biological activities, the animal studies were approved by the Institutional Animal Ethics Committee (IAEC) of Roland Institute of Pharmaceutical Sciences, Berhampur (Ethical approval number: 926/PO/RE/S/06/CPCSEA). The acute oral toxicity followed the OECD-423 guideline prior to selecting safe/non-toxic doses for further *in vivo* analgesic and anti-inflammatory investigation [42,43]. A total of two compounds (**4a** and **5e**) based on computational analyses were selected using healthy Wistar albino rats of either sex (150-200 g) in three different concertation: 50, 100, 200, 400 and 800 mg/kg. The test compounds were administered orally and the animals were observed for 14 days to monitor mortality, behavioural changes and any signs of toxicity.

The analgesic potential of **4a** and **5e** was evaluated in Wistar albino rats using Eddy's hot plate method [44,45]. Rats were randomly divided into six groups (n = 6). Group I received distilled water (control), Group II received penta-

zocine (standard) and Groups III-VI received the test compounds in two fix doses (200 and 400 mg/kg p.o.). The potency was recorded from two different methods *viz*. antinociceptive effect onset concentration (AEOC) and minimum effective occlusive concentration (MEOC) at doses of 200 and 400 mg/kg (p.o.), where pentazocine (PTZ) 10 mg/kg was used as reference standard. Each animal was put on an aluminum hot plate that was kept at 55 ± 0.5 ºC and the time it took for them to lick their paws or jump was recorded. Measurements were taken at 30, 60, 90, 120, 180 and 240 min post-administration. A cut-off time of 15 sec was maintained to prevent tissue injury.

Anti-inflammatory and antioxidant activity: The anti-inflammatory potential of two lead compounds **4a** and **5e** was evaluated using two approaches *viz*. the *in vitro* protein denaturation assay (hot and cold water extracts) and the *in vivo* carrageenan-induced paw edema model [46,47]. For *in vitro* studies, ~0.2 g of each synthesized compound was dispersed in 20 mL of distilled water. Hot water extracts were prepared by heating at 80 ºC for 30 min after 15 min equilibration at room temperature, while cold extracts were prepared by incubating at 10 ºC for 60 min. Both were filtered and dried. Prednisolone and ibuprofen served as reference drugs (0.2 g/20 mL distilled water). Serial dilutions (1000-0.01 µg/mL) of test and reference samples were prepared in 5 mL volumes containing 2.8 mL phosphate buffer (pH 6.4), 0.2 mL fresh egg albumin and 2 mL test solution. Distilled water served as a control. Reaction mixtures were incubated at 37 ± 2 ºC for 20 min, then heated at 70 ºC for 5 min to induce protein denaturation, cooled to room temperature and absorbance measured at 680 nm. Each test was conducted three times and the percentage inhibition of protein denaturation was calculated using the following formula:

$$\text{Inhibition (\%)} = \left(\frac{A_c - A_t}{A_c}\right) \times 100$$

where A_c = absorbance of control and A_t = absorbance of test sample.

Alongside, anti-inflammatory activity was evaluated using the carrageenan-induced paw edema method in Wistar albino rats [47,48]. Acute inflammation was induced by sub-plantar injection of 0.1 mL of 1% freshly prepared carrageenan suspension into the right hind paw of each rat. Paw volumes of both injected and contralateral paws were recorded at 0, 30, 60, 120, 180 and 240 min using a plethysmometer. Briefly, animals were divided into five groups (n = 6). Group I received distilled water (10 mL/kg, p.o.) and served as a control, Group II received indomethacin (5 mg/kg, p.o.) as a standard and Groups III-V received the synthesized test compounds at doses of 200 and 400 mg/kg (p.o.). The percentage inhibition of paw edema was calculated using the following formula:

$$I\ (\%) = 100 \times \left(1 - \frac{(a - x)}{(b - y)}\right)$$

where a = mean paw volume of test/standard after carrageenan administration; b = mean paw volume of control after carrageenan administration; x = mean paw volume of test/standard before carrageenan administration; and y = mean paw volume of control before carrageenan administration.

Similarly, the antioxidant potential of **4a** and **5e** was determined using the DPPH (2,2-diphenyl-1-picrylhydrazyl) assay method [38,49]. Briefly, DPPH solution was prepared in ethanol solvent (4 mg in 100 mL of ethanol), where ascorbic acid (10 mg/mL DMSO) was used as a reference standard for the study. All synthesized products at different concentrations ranging from 50, 100, 200 and 400 mg/mL were mixed with 2.96 mL of freshly prepared DPPH solution and incubated in the dark at room temperature for 20 min. Absorbance of the reaction mixture was measured at 517 nm using a UV/Vis spectrophotometer and the radical scavenging activity (RSA) was calculated using the following equation:

$$\text{RSA (\%)} = \frac{A_{control} - A_{sample}}{A_{control}} \times 100$$

where $A_{control}$ is the absorbance of control (DPPH + ethanol) and A_{sample} is the absorbance of test sample (DPPH + compound solution).

All the experimental results were expressed as mean ± standard. Data obtained from different groups in analgesic, anti-inflammatory and antioxidant studies were subjected to statistical evaluation [34,44]. Comparisons between test compounds, standard drugs and control groups were analyzed using one-way analysis of variance (ANOVA) followed by the post-hoc Tukey's multiple comparison test, while independent sample *t*-tests were used where applicable. A *p*-value of less than 0.05 was considered statistically significant. Statistical analyses were performed using GraphPad Prism 8.0 software.

Computational investigations

Target-selection and molecular docking study: After synthesis and characterization, a computer-aided drug design (CADD) platform was employed to explore target-specific efficacy and drug-likeness before selecting lead compounds for *in vitro* and *in vivo* studies, providing a cost-effective approach compared with the traditional trial-and-error drug discovery process [38,39]. To investigate target-specific activity, cyclooxygenase-2 (COX-2), a well-established therapeutic target, was selected [38,50]. This enzyme plays a crucial role in inflammation, oxidative stress and pain signalling, making it a relevant target for therapeutic investigation [50-52]. Based on our hypothesis, COX-2 was selected to assess the antioxidant, analgesic and anti-inflammatory potential of the proposed candidates [30,50,53]. For the docking study, the crystallographic structure of COX-2 was retrieved from the Protein Data Bank (PDB ID: 5F1A). Ligand structures were optimized using the Merck Molecular Force Field 94 (MMFF94). Molecular docking was performed using AutoDock 4.2 following the previously reported protocol and default parameters, with a grid box defined around the active-site residues [38,39]. Protein-ligand interactions were visualized using BIOVIA Discovery Studio Visualizer [38].

Physico-chemical, pharmacokinetics and HOMO-LUMO analyses: The physico-chemical properties of the synthesized derivatives were assessed using SwissADME, covering Lipinski's rule of five (Ro5), bioavailability (BA), gastrointestinal (GI) absorption, blood–brain barrier (BBB) permeability, P-glycoprotein substrate affinity, cytochrome P450 inhibitory potential and skin permeation (Log Kp) [38,39].

Drug-likeness (DL) scores were determined with Molsoft by comparing the chemical structures with its training set datasets [38,39]. Frontier molecular orbital calculations were performed to examine the electronic properties and structural characteristics of the derivatives through the highest occupied molecular orbital (HOMO) and lowest unoccupied molecular orbital (LUMO) energies [38]. HOMO–LUMO energies were calculated using Avogadro 1.95-ORCA with the Restricted Hartree-Fock (RHF) method [38,39].

RESULTS AND DISCUSSION

A series of 1,2,4-triazole-3-yl-sulfanyl-acetamide derivatives (**4a-e** and **5a-e**) was synthesized through the designed routes presented in **Schemes I** and **II**. Both routes employed a common scaffold, with different R-groups introduced at defined positions to generate structural diversity. The optimized reactions afforded yields above 60%, supporting the reproducibility of the synthetic methodology. The derivatives were characterized by melting-point analysis, FTIR, ^{1}H NMR, ^{13}C NMR and mass spectrometry.

For compound **4a** (Fig. 1a), DSC displayed a sharp endothermic event at 163.50 ºC (onset 154.37 ºC; ΔH = -49.62 J/g), consistent with crystal melting. The narrow transition range (ΔT = 9.22 ºC) is compatible with a highly crystalline material. Endothermic events at 45.09 and 87.94 ºC may arise from moisture and residual solvent, respectively, with no corresponding TGA mass loss above 100 ºC. No exothermic event was observed below 180 ºC. The DSC profile of compound **5e** (Fig. 1b) contained three endothermic events. A broad peak at 122.65 ºC (onset 108.94 ºC; ΔH = -120.66 J/g) was assigned to residual solvent loss. A sharper transition at 161.78 ºC (onset 155.12 ºC; ΔH = -24.24 J/g) corresponded to melting of crystalline **5e**. No exothermic event occurred below 170 ºC, which indicate that the solid-state stability within the investigated temperature range.

Spectroscopic data for compounds **4a-e** and **5a-e** supported the assigned structures. FTIR spectra contained characteristic –NH, C=O and C–S stretching bands, while ^{1}H NMR spectra displayed signals attributable to aromatic protons, triazole protons and methylene groups. Molecular-ion signals in the mass spectra were consistent with the calculated molecular masses.

Computational studies: Molecular docking was performed to assess the binding behaviour of the synthesized derivatives (**4a-e** and **5a-e**) toward COX-2, with indomethacin used as the reference ligand. Derivatives **4a-e** show docking scores between -10.68 and -12.09 kcal/mol. Compounds **4a** (-12.09 kcal/mol) and **4b** (-12.02 kcal/mol) showed the most favourable scores within this series and were more negative than the indomethacin score of -11.05 kcal/mol. Derivatives **5a-e** show a wider range of -9.44 to -13.15 kcal/mol, with **5d** and **5e** giving the most negative values. The numerical scores should be interpreted cautiously as grid-based docking functions commonly carry an uncertainty of approximately 2-3 kcal/mol; the values alone cannot establish superior thermodynamic affinity over the reference ligand.

The protein-ligand interaction analysis provided a complementary basis for lead prioritization. The synthesized derivatives formed 5-14 contacts with residues within the COX-2 binding region (Table-1). The COX-2-**4a** complex displayed 10 residue contacts involving Cys36, His39, Arg44, Val46, Cys47, Tyr130, Ala151, Leu152, Pro153 and Pro156 (Fig. 2a). Compound **5e** engaged 13 residues: Cys36, His39, Arg44, Val46, Cys47, Tyr130, Gly135, Ala151, Leu152, Pro153, Pro154, Pro156 and Asp157 (Fig. 2b). Indomethacin formed eight contacts with Asn34, Cys36, Cys41, Cys47, Cys49, Pro153, Pro154 and Pro156 (Fig. 2c). The broader interaction networks observed for compounds **4a** and **5e**, together with their favourable biological profiles, supported their selection for experimental validation. Although compound **5e** had the most negative docking score (-13.15 kcal/mol), its selection was based on the combined interaction pattern and structural complementarity rather than the docking score alone.

The physico-chemical assessment revealed that the **4a-e** derivatives satisfied Lipinski's Rule of Five, whereas several **5a-e** compounds deviated from the preferred parameters, mainly due to their higher molecular weights (Table-2). The predicted bioavailability score averaged 0.55, a value compatible with several marketed drugs. Positive drug-likeness (DL) scores were obtained for all derivatives. Compound **4b** had the highest DL score (1.16), while compound **5d** gave the highest value in **Scheme-II** (1.05). The selected leads **4a** and **5e** had DL scores of 0.60 and 0.68, respectively, supporting their further evaluation.

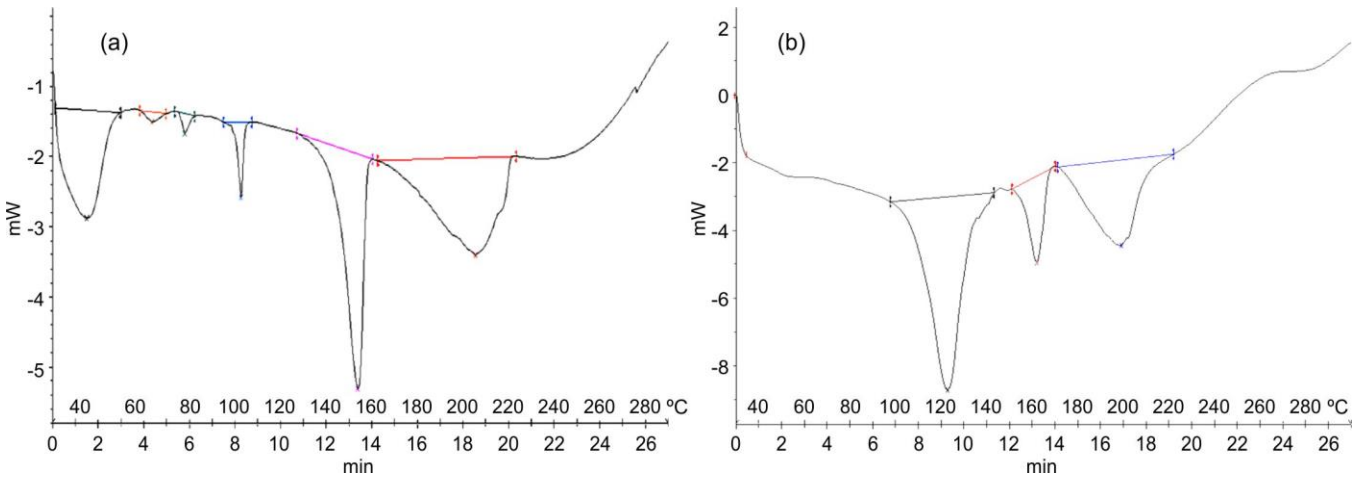

Fig. 1. DSC curves of (a) **4a** and (b) **5e** at 10 ºC min^{-1} under N_2 atmosphere

TABLE-1
MOLECULAR DOCKING SCORE (kcal/mol) OF DERIVATIVES ALONG WITH REFERENCE STANDARD INDOMETHACIN AGAINST COX2 WITH THEIR INTERACTIONS

Compound	Docking score	Interactive amino acids recoded for protein-ligand docking complexes through BIOVIA-Discovery studio visualizer
4a	-12.09	Cys36, His39, Arg44, Val46, Cys47, Tyr130, Ala151, Leu152, Pro153, Pro156
4b	-12.02	Cys36, His39, Cys41, Arg44, Val46, Cys47, Tyr130, Ala151, Leu152, Pro153, Pro156
4c	-10.85	Cys36, Cys41, Arg44, Gly45, Val46, Cys47, Tyr130, Gly135, Ala151, Leu152, Pro153, Pro156, Gln461, Arg469
4d	-11.39	Asn43, Arg44, Pro153, Lys468, Met471
4e	-10.68	Cys41, Arg44, Leu152, Pro153, Lys468, Met471
5a	-9.44	Leu80, Pro153, Lys 468
5b	-10.57	Cys36, Arg44, Val46, Cys47, Asp125, Tyr130, Leu152, Pro153, Pro156
5c	-9.51	Lys79, Lys83, Pro84, Pro86, Tyr115, Met471
5d	-13.04	His207, Lys211, His214, Val291, Asn382, His386, Leu391
5e	-13.15	Cys36, His39, Arg44, Val46, Cys47, Tyr130, Gly135, Ala151, Leu152, Pro153, Pro154, Pro156, Asp157
*Indomethacin	-11.05	Asn34, Cys36, Cys41, Cys47, Cys49, Pro153, Pro154, Pro156

*Reference standard

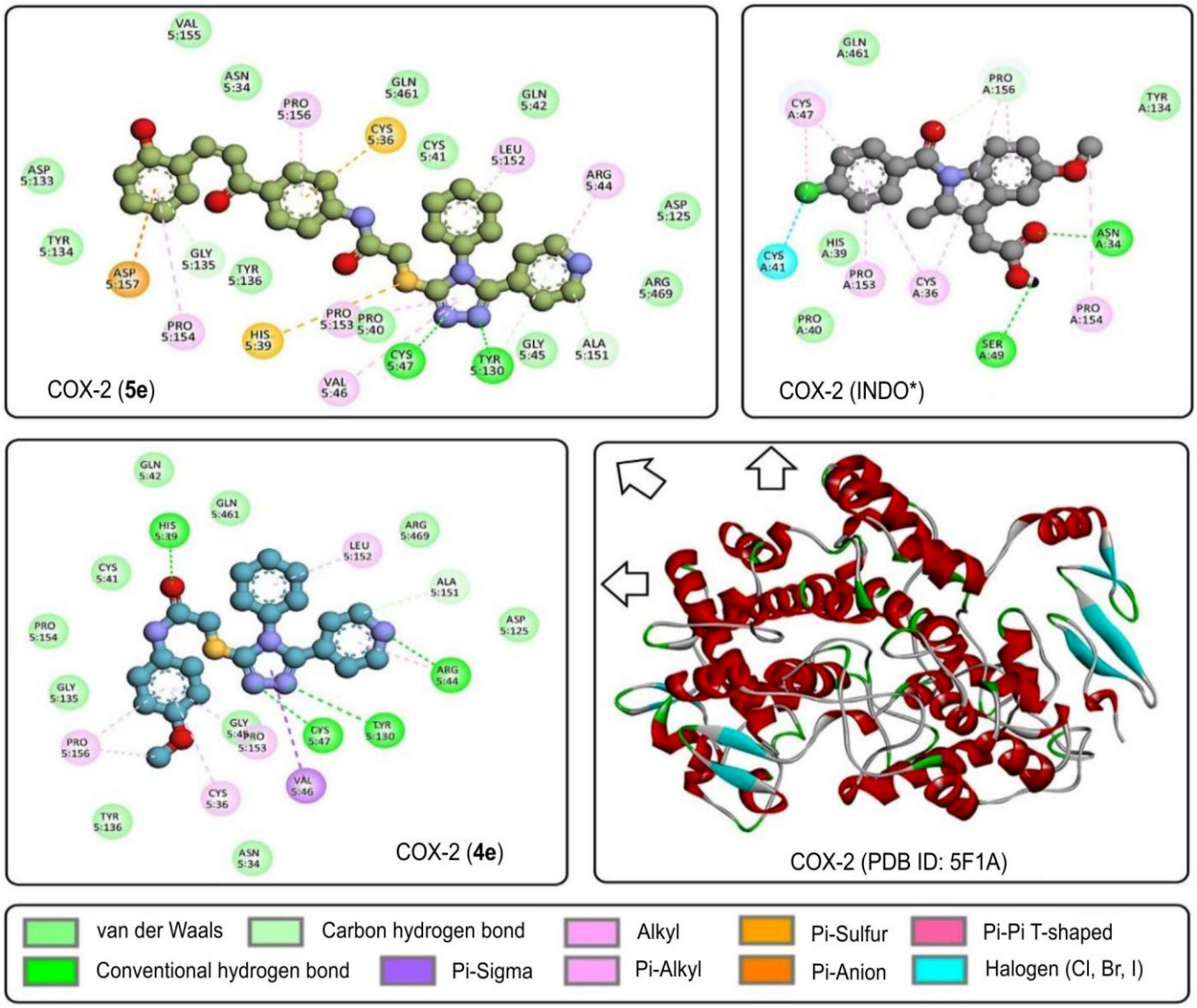

Fig. 2. Protein–ligand interaction profiles of COX-2 with two selected potential derivatives based on docking score along with the reference drug in 2D interaction view. The panels illustrate the binding interactions of COX-2 with **4a**, COX-2 with **5e** and COX-2 with indomethacin (the reference standard)

TABLE-2
PHYSIOCHEMICAL AND HOMO-LUMO, ENERGY GAP (eV) OF SYNTHETIZED COMPOUNDS

Compd.	Lipinski Rule of Five	Bioavailability score	Drug-likeness score	LUMO energy	HOMO energy	Energy gap (ΔE_{H-L} eV)
4a	Yes	0.55	0.60	1.915	-8.070	9.985
4b	Yes	0.55	1.16	1.856	-8.595	10.451
4c	Yes	0.55	0.92	1.823	-8.681	10.504
4d	Yes	0.55	0.27	1.017	-9.188	10.205
4e	Yes	0.55	0.08	1.825	-8.810	10.635
5a	No	0.55	0.70	1.722	-8.791	10.513
5b	No	0.55	0.94	1.781	-8.361	10.142
5c	No	0.55	0.50	1.134	-9.038	10.172
5d	No	0.55	1.05	1.602	-8.810	10.412
5e	No	0.55	0.68	1.510	-8.476	9.986

The predicted pharmacokinetic profiles differed between the two series (Table-3). Most of the **4a-e** derivatives showed high gastrointestinal absorption, with **4e** as the exception, whereas the **5a-e** derivatives were predicted to have low GI absorption. None of the derivatives was predicted to readily cross the blood–brain barrier, a profile considered favourable for the intended peripheral therapeutic application. The compounds were predicted to lack significant P-glycoprotein substrate behaviour, while their cytochrome-related interactions and skin-permeation (Log Kp) values varied according to molecular structure.

Frontier molecular orbital analysis provided further information on the electronic properties of the derivatives. The HOMO and LUMO distributions were associated with functional regions capable of participating in molecular interactions. The HOMO–LUMO gaps of **4a** (9.985 eV) and **5e** (9.986 eV) were closely comparable and among the more favourable values observed for the series (Tables 2 and 4). A relatively smaller HOMO–LUMO gap is generally associated with higher electronic softness and charge-transfer propensity, which may favour molecular recognition and interaction with a protein binding site.

The CADD assessment identified **4a** and **5e** as lead compounds from **Schemes I** and **II**, respectively. Their selection was based on docking scores, residue-level interaction patterns, drug-likeness, predicted ADME characteristics and frontier molecular orbital properties. These computational findings served as a prioritization tool for subsequent *in vitro* and *in vivo* evaluation within the resource-limited experimental framework.

Biological activities: Acute oral toxicity of the two lead compounds **4a** and **5e**, was assessed at 50, 100, 200, 400 and 800 mg/kg according to OECD-423 guidelines. During the 14 day observation period, neither compound caused mortality or marked behavioural or physiological changes at doses up to 400 mg/kg. At 800 mg/kg, abnormalities appeared after six days, limiting the use of this dose for subsequent experiments. Based on the safety observations, 200 and 400 mg/kg were selected for the *in vivo* efficacy studies. Analgesic activity was examined at both doses using the MEOC and AEOC methods, with responses recorded at predefined time intervals (Table-5). The pentazocine group exhibited slightly better activity at the lower dose of 10 mg/kg, whereas the distilled-water control showed the weakest response. At 200 and 400 mg/kg, compounds **4a** and **5e** displayed analgesic effects approaching those of pentazocine.

The *in vitro* anti-inflammatory activity was assessed by protein-denaturation assays under cold- and hot-water conditions. The IC_{50} values of the reference drugs ibuprofen and prednisolone were determined and the corresponding results for compounds **4a** and **5e** are shown in Tables 5 and 6. Both compounds exhibited concentration-dependent inhibition of protein denaturation and showed higher activity than the reference drugs under the tested conditions. The findings are consistent with protein-stabilizing and membrane-protective effects, supporting their anti-inflammatory potential.

TABLE-3
PREDICTED PHARMACOKINETICS PROFILE OF SYNTHETIZED COMPOUNDS

Compd.	GI-abr.	BBB (yes/no)	P-gps (yes/no)	CYP1A2 inhibitor	CYP2C19 inhibitor	CYP2C9 inhibitor	CYP2D6 inhibitor	CYP3A4 inhibitor	Log K_p (cm/s)
4a	High	No	No	No	Yes	Yes	Yes	Yes	-6.43
4b	High	No	No	Yes	Yes	Yes	Yes	Yes	-6.00
4c	High	No	No	Yes	Yes	Yes	Yes	Yes	-6.27
4d	Low	No	No	No	Yes	Yes	No	Yes	-3.24
4e	High	No	No	Yes	Yes	Yes	Yes	Yes	-6.22
5a	Low	No	No	No	Yes	Yes	No	Yes	-5.77
5b	Low	No	No	No	Yes	Yes	No	No	-6.12
5c	Low	No	No	No	Yes	Yes	No	Yes	-6.17
5d	Low	No	No	No	Yes	Yes	No	Yes	-5.54
5e	Low	No	No	No	Yes	Yes	No	No	-6.12

BBB = Blood-brain barrier; Log K_p (skin permeation); P-gps, P-gp substrate

TABLE-4
GRAPHICAL PRESENTATION OF HOMO-LUMO ENERGY PLOTS OF SYNTHESIZED COMPOUNDS

Compound	LUMO energy plot	HOMO energy plot
4a	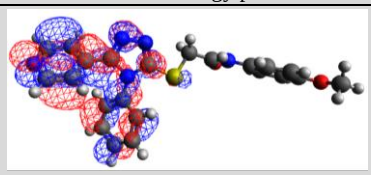	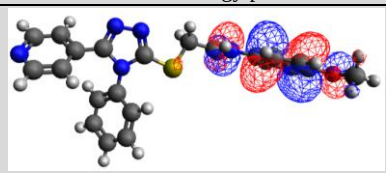
4b	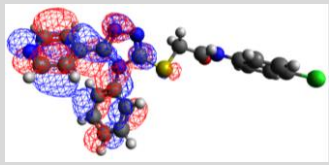	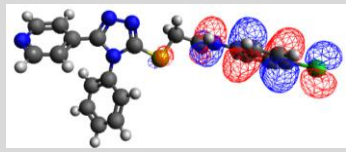
4c	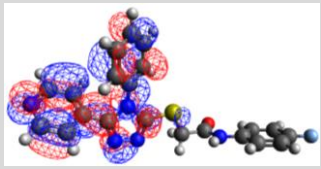	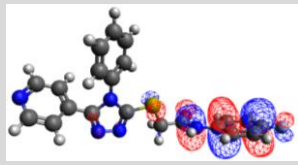
4d	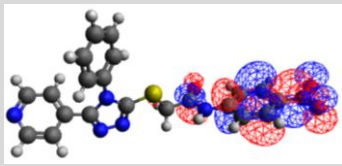	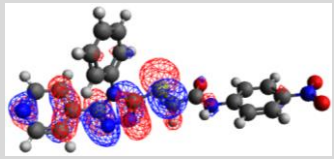
4e	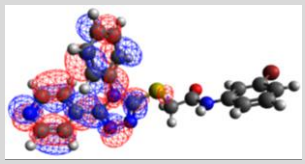	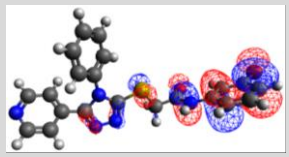
5a	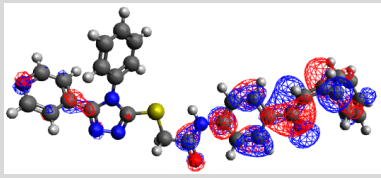	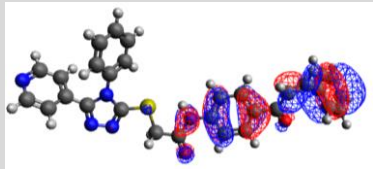
5b	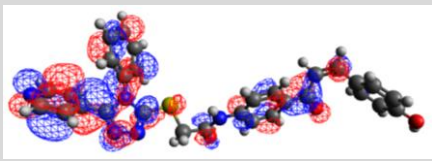	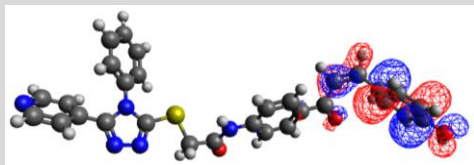
5c	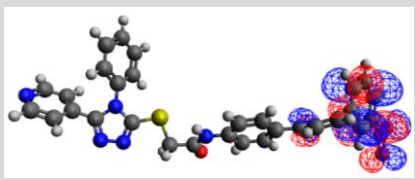	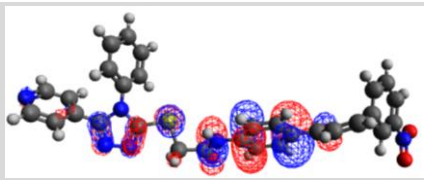
5d	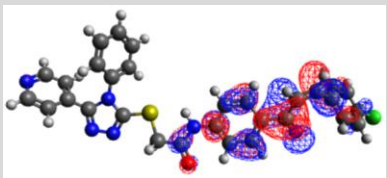	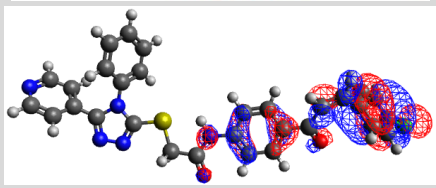
5e	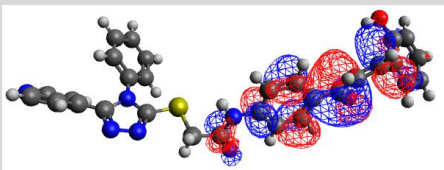	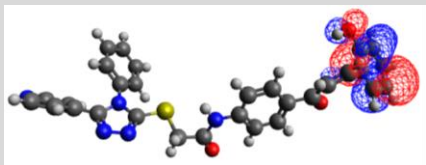

TABLE-5
ANALGESIC POTENCY OF **4a** AND **5e** FROM MEOC AND AEOC METHOD AT DIFFERENT TIME INTERVAL (30 TO 240 min)

Drugs/ potency	Distilled water	**4a** in MEOC (mg/kg)		**4a** in AEOC (mg/kg)		**5e** in MEOC (mg/kg)		**5e** in AEOC (mg/kg)		PTZ* (mg/kg)
Doses	0.5	200	400	200	400	200	400	200	400	10
Mean BT (sec.)	4.28 ± 0.018	4.60 ± 0.035	4.33 ± 0.036	4.88 ± 0.051	5.12 ± 0.031	4.71 ± 0.023	4.19 ± 0.037	4.74 ± 0.026*	4.19 ± 0.013	4.41 ± 0.036
30 min	4.17 ± 0.187	6.88 ± 0.031	6.94 ± 0.028	7.02 ± 0.032	7.54 ± 0.024	6.85 ± 0.038	6.91 ± 0.057	7.27 ± 0.013	7.58 ± 0.013	7.69 ± 0.042*
60 min	4.69 ± 0.029	7.19 ± 0.036	7.49 ± 0.024	8.08 ± 0.025	8.29 ± 0.037	7.09 ± 0.043	7.47 ± 0.028	8.14 ± 0.012	8.22 ± 0.316	8.62 ± 0.026*
90 min	4.76 ± 0.042	8.44 ± 0.043	8.93 ± 0.051	8.92 ± 0.044*	9.17 ± 0.039	8.61 ± 0.028	8.98 ± 0.040	9.19 ± 0.015	9.38 ± 0.011	9.46 ± 0.048*
120 min	4.16 ± 0.036	10.93 ± 0.045	11.01 ± 0.023	10.99 ± 0.037	11.03 ± 0.028	10.68 ± 0.035	10.92 ± 0.020	11.00 ± 0.009	11.10 ± 0.014	11.14 ± 0.039*
180 min	4.02 ± 0.048	9.69 ± 0.043	9.71 ± 0.021	9.79 ± 0.046	9.82 ± 0.041	9.68 ± 0.039	9.99 ± 0.032	10.06 ± 0.022	10.13 ± 0.011	10.69 ± 0.039*
240 min	4.56 ± 0.036	8.38 ± 0.021	8.75 ± 0.028	8.92 ± 0.032	9.21 ± 0.046*	8.18 ± 0.031	8.45 ± 0.034	9.38 ± 0.021	9.86 ± 0.015*	9.95 ± 0.042*

*Standard drug; BT = basal time; PTZ = pentazocine.

TABLE-6
ANTI-INFLAMMATORY POTENCY OF **4a** AND **5e** IN *in vitro* PROTEIN DENATURATION USING THE COLD AND HOT WATER METHODS

Conc. (μg/mL)	Percent of inhibition of **4a**		Percent of inhibition of **5e**		Percent of inhibition of standard drugs	
	Cold water	Hot water	Cold water	Hot water	Ibuprofen (std.)	Prednisolone (std.)
0.01	12.26 ± 0.96	19.27 ± 1.34	14.13 ± 3.56	20.43 ± 0.14	16.13 ± 3.56	5.43 ± 0.14
0.1	15.30 ± 0.93	20.58 ± 0.62	16.09 ± 0.44	21.95 ± 1.05	13.09 ± 0.44	5.95 ± 1.05
1	21.43 ± 1.49	20.61 ± 0.66	22.71 ± 0.51	20.69 ± 1.04	12.71 ± 0.51	6.03 ± 1.04
10	23.74 ± 0.75	22.41 ± 1.32	23.29 ± 4.27	22.49 ± 1.04	11.28 ± 4.27	6.21 ± 1.04
100	26.09 ± 2.27	23.71 ± 3.36	27.16 ± 1.96	23.79 ± 1.51	11.12 ± 1.96	6.47 ± 1.51
1000	28.71 ± 0.72	27.64 ± 0.73	28.77 ± 1.11	27.83 ± 1.51	8.57 ± 1.10	8.83 ± 1.51

The *in vivo* anti-inflammatory response was evaluated using the paw-edema model, with indomethacin serving as the reference drug (Table-7). The control and reference groups exhibited higher paw swelling than the compound-treated groups. Both compounds **4a** and **5e** reduced edema in a dose-dependent manner, with the 400 mg/kg dose giving the stronger response. These results support the anti-inflammatory activity observed in the *in vitro* protein-denaturation assay.

Radical-scavenging capacity was measured by the DPPH assay. Compound **4a** showed moderate-to-good activity at 100 ppm, with 39.42% scavenging compared with ascorbic acid (Table-8). Compound **5e**, exhibited approximately 40% scavenging at the same concentration and performed better than the corresponding compound **4a** (Table-9). Both compounds displayed concentration-dependent radical-scavenging activity. The DPPH results provide an independent measure of chemical radical-scavenging capacity and complement the anti-inflammatory findings. Within the tested safety range, both leads exhibited favourable biological activity, with compound **5e** displaying the stronger combined activity profile.

SAR studies: Selection of the 1,2,4-triazole nucleus and sulfanyl-acetamide linkage was guided by the pharmacological relevance of these structural motifs and their occurrence in FDA-approved drugs, providing a rational basis for the proposed molecular design. The SAR analysis points to an key role for phenyl-ring substitution in modulating biological activity. In the hot-plate assay, 2- and 4-chloro, 3-nitro, 4-bromo, 4-hydroxy, 4-methoxy and 2,4-dimethoxy substituents were

TABLE-7
THE *in vivo* ANTI-INFLAMMATORY POTENCY OF **4a** AND **5e** WAS EVALUATED IN THE PAW EDEMA METHOD AT DIFFERENT TIME INTERVALS IN AN ACUTE INFLAMMATION STUDY

Drugs/potency	Distilled water	**4a** in MEOC (mg/kg)		**4a** in AEOC (mg/kg)		Indomethacin (std.) (mg/kg)
Doses	0.5 mL	200	400	200	400	5
30 min	0.29 ± 0.052	0.25 ± 0.026	0.20 ± 0.058*	0.26 ± 0.018	0.23 ± 0.01*	0.19 ± 0.032*
60 min	0.42 ± 0.051	0.34 ± 0.014	0.28 ± 0.039*	0.37 ± 0.016	0.29 ± 0.026*	0.24 ± 0.014*
120 min	0.68 ± 0.061	0.52 ± 0.005	0.43 ± 0.048*	0.55 ± 0.015	0.44 ± 0.016*	0.35 ± 0.017*
180 min	0.87 ± 0.062	0.69 ± 0.007	0.54 ± 0.055*	0.72 ± 0.018	0.58 ± 0.014*	0.46 ± 0.021*
240 min	0.78 ± 0.054	0.61 ± 0.018	0.47 ± 0.037*	0.65 ± 0.024	0.50 ± 0.018*	0.39 ± 0.016*

*$p < 0.05$

TABLE-8
ANTIOXIDANT ACTIVITY DATA OF SYNTHESIZED COMPOUND **4a**

DPPH (ppm)	Control	Sample conc. (mM)	Absorbance	%RSA	IC_{50}
100	0.52	0.06	0.315	39.4230769	1907
200	0.52	0.12	0.300	42.3076923	4965
400	0.52	0.24	0.243	53.2692308	11081
500	0.52	0.30	0.220	57.6923077	14139
700	0.52	0.42	0.214	58.8461538	20255
1000	0.52	0.60	0.160	69.2307692	29430
Ascorbic acid	0.014	0.058	82%	100	

TABLE-9
ANTIOXIDANT ACTIVITY OF
SYNTHESIZED COMPOUND **5e**

DPPH (ppm)	Control	Absorbance	%RSA	IC_{50}
100	0.52	0.312	40.0	1122
200	0.52	0.291	44.0	2803
400	0.52	0.228	56.2	6164
500	0.52	0.18	65.4	7845
700	0.52	0.14	73.1	11206
1000	0.52	0.035	93.3	16248
Ascorbic acid	0.014	0.058	82%	–

associated with enhanced activity. Electron-withdrawing groups such as 2-chloro, 4-chloro, 3-nitro and 4-bromo gave stronger inhibition than the unsubstituted analogues [54,55]. Such substituents may influence interactions with inflammatory mediators or improve accommodation within the COX-2 binding site.

Electron-donating methoxy and hydroxy groups can support hydrogen-bond formation and maintain activity across the biological assays. The corresponding derivatives exhibited edema inhibition within the range observed for the reference indomethacin (50-70%). The 4-halo derivatives consequently emerge as useful structural candidates for combined analgesic and anti-inflammatory activity. Sulfur within the thioacetamide linkage may contribute to radical stabilization, while 4-chloro, 4-bromo and 3-nitro substituents were associated with stronger analgesic and edema-inhibitory responses [54,56]. The thioacetamide bridge may participate in hydrogen donation during DPPH radical scavenging at 100 µg/mL, whereas electron-donating groups such as –OH and –OMe can provide complementary hydrogen-bonding interactions. The combined structural features may account for the balanced activity observed for compound **5e**.

The SAR pattern further distinguishes the simple aryl derivative **4a** from the chalcone-extended derivatives **5a** and **5e**. Introduction of the *ortho*-hydroxy group in **5e** is particularly relevant to its activity profile, providing a structural feature capable of hydrogen donation and additional intermolecular interactions. The resulting molecular architecture may favour simultaneous radical scavenging and interactions associated with inflammatory and nociceptive pathways. Among the tested derivatives, **5e** displayed the most favourable combination of antioxidant, analgesic and anti-inflammatory responses.

The study integrates pharmacophore-based design, CADD assisted lead selection and experimental validation, allowing the investigation to focus on two lead candidates within a resource-limited setting [38,39]. The activity profiles and drug like characteristics of **4a** and **5e** support their consideration as preliminary lead structures for further optimization, particularly toward safer anti-inflammatory agents with complementary analgesic activity [38]. Their translational relevance remains preliminary, as the study is limited to selected *in vitro* and *in vivo* models.

The DPPH assay provides evidence of chemical radical-scavenging capacity rather than a direct measure of antioxidant activity mediated through COX-2. Compound **4a** displayed concentration-dependent scavenging at low concentration, while compound **5e** gave the stronger response under the tested conditions. From an SAR perspective, the multifunctional profile of these derivatives may arise from two complementary properties: interaction with the COX-2 active site and chemical neutralization of free radicals through suitable substituents and the sulfanyl-acetamide linkage. The relationship between inflammation and oxidative stress provides a biological context for these findings, but the DPPH data should not be interpreted as evidence of an intrinsic antioxidant mechanism associated with COX-2 inhibition. On the basis of the combined experimental and computational findings, compound **5e** represents the more promising lead for subsequent mechanistic, pharmacokinetic and therapeutic investigations.

Conclusion

In the present study, 10 novel 1,2,4-triazole-3-yl-sulfanyl-acetamide derivatives (**4a-e** and **5a-e**) were synthesized and structurally characterized using spectroscopic techniques. A CADD-based screening strategy was applied before *in vivo* studies to prioritize lead candidates and optimize experimental resources. Compounds **4a** and **5e** exhibited promising anti-inflammatory activity in both *in vitro* and *in vivo* models, accompanied by analgesic and antioxidant effects. The combined *in silico*, *in vitro* and *in vivo* findings identify **4a** and **5e** as promising multifunctional leads. Further pharmacological, mechanistic and preclinical studies are warranted to establish their therapeutic potential.

ACKNOWLEDGEMENTS

This research forms part of the Ph.D. thesis of Mr. Santanu Kumar Hotta, School of Pharmaceutical Sciences (Regd. No. 2281606017), Siksha 'O' Anusandhan Deemed to be University, Bhubaneswar, India. The authors sincerely acknowledge the support and cooperation extended by the authorities and staff of the participating institutions during the course of this

study. The authors gratefully acknowledge CSIR-CSMCRI, Bhavnagar, India, for providing NMR spectral analysis facilities; Roland Institute of Pharmaceutical Sciences, Berhampur, for providing FTIR spectral analysis and facilities for animal experimentation and Department of Pharmaceutical Analysis, Siksha 'O' Anusandhan Deemed to be University, Bhubaneswar, for providing facilities for DSC analysis.

CONFLICT OF INTEREST

The authors declare that there is no conflict of interests regarding the publication of this article.

DECLARATION OF AI-ASSISTED TECHNOLOGIES

During the preparation of this manuscript, the authors used an AI-assisted tool(s) to improve the language and no data, results or scientific conclusions were generated by AI. All analyses, interpretations and conclusions are the authors' own. The authors reviewed and edited the content and take full responsibility for the published work.

REFERENCES

1. B.P. Smith and S.M. Huang, *Clin. Pharmacol. Ther*., **97**, 196 (2015); https://doi.org/10.1002/cpt.62
2. J.G. Moffat, F. Vincent, J.A. Lee, J. Eder and M. Prunotto, *Nat. Rev. Drug Discov*., **16**, 531 (2017); https://doi.org/10.1038/nrd.2017.111
3. L. Wang, Z. Zhou, X. Yang, S. Shi, X. Zeng and D. Cao, *Drug Discov. Today*, **29**, 103985 (2024); https://doi.org/10.1016/j.drudis.2024.103985
4. I.B. Campbell, S.J.F. Macdonald and P.A. Procopiou, *Drug Discov. Today*, **23**, 219 (2018); https://doi.org/10.1016/j.drudis.2017.10.007
5. S.S. Swain, S.K. Paidesetty, R.N. Padhy and T. Hussain, *Chem. Biol. Drug Des*., **96**, 714 (2020); https://doi.org/10.1111/cbdd.13685
6. A. Wahi, M. Bishnoi, N. Raina, M.A. Singh, P. Verma, P.K. Gupta, G. Kaur, H.S. Tuli and M. Gupta, *Oncol. Res*., **32**, 19 (2023); https://doi.org/10.32604/or.2023.042228
7. C. Zobi and O. Algul, *Chem. Biol. Drug Des*., **105**, e70045 (2025); https://doi.org/10.1111/cbdd.70045
8. S. Kumari, A.V. Carmona, A.K. Tiwari and P.C. Trippier, *J. Med. Chem*., **63**, 12290 (2020); https://doi.org/10.1021/acs.jmedchem.0c00530
9. G. Li Petri, M.V. Raimondi, V. Spanò, R. Holl, P. Barraja and A. Montalbano, *Top. Curr. Chem.*, **379**, 34 (2021); https://doi.org/10.1007/s41061-021-00347-5
10. N. Upadhyay, K. Tilekar, F. Loiodice, N.Y. Anisimova, T.S. Spirina, D.V. Sokolova, G.B. Smirnova, J.Y. Choe, F.J. Meyer-Almes, V.S. Pokrovsky, A. Lavecchia and C.S. Ramaa, *Bioorg. Chem*., **107**, 104527 (2021); https://doi.org/10.1016/j.bioorg.2020.104527
11. A. Acharya, M. Yadav, M. Nagpure, S. Kumaresan and S.K. Guchhait, *Drug Discov. Today*, **29**, 103845 (2024); https://doi.org/10.1016/j.drudis.2023.103845
12. N. Parvin, M. Aslam, M.N. Alam and T.K. Mandal, *Nanomaterials*, **15**, 1733 (2025); https://doi.org/10.3390/nano15221733
13. R.M. Lu, H.L. Chiang, J.P. Yuan, H.H. Wang, C.Y. Chen, S.S. Panda, K.H. Liang, H.P. Peng, S.H. Ko, H.J. Hsu, M. Kumari, Y.J. Su, Y.T. Tse, N.L. Chou and H.C. Wu, *J. Biomed. Sci*., **32**, 98 (2025); https://doi.org/10.1186/s12929-025-01190-2
14. L. Lombardi, V.D. Genio, F. Albericio and D.R. Williams, *Chem. Rev*., **125**, 7099 (2025); https://doi.org/10.1021/acs.chemrev.4c00989
15. D. Becerra, R. Abonia and J.C. Castillo, *Molecules*, **27**, 4723 (2022); https://doi.org/10.3390/molecules27154723
16. O.F. Elebiju, O.O. Ajani, G.O. Oduselu, T.A. Ogunnupebi and E. Adebiyi, *Front. Chem.*, **10**, 1074331 (2023); https://doi.org/10.3389/fchem.2022.1074331
17. A. Kumar, A. Kaushal, P.K. Verma, M.K. Gupta, G. Chandra, U. Kumar, A.K. Yadav and D. Kumar, *Eur. J. Med. Chem*., **280**, 116896 (2024); https://doi.org/10.1016/j.ejmech.2024.116896
18. G. Kumari, S. Dhillon, P. Rani, M. Chahal, D.K. Aneja and M. Kinger, *ACS Omega*, **9**, 18709 (2024); https://doi.org/10.1021/acsomega.3c10299
19. M. Ward and N.M. O'Boyle, *RSC Med. Chem*., **16**, 4540 (2025); https://doi.org/10.1039/D5MD00403A
20. R. Aggarwal and G. Sumran, *Eur. J. Med. Chem*., **205**, 112652 (2020); https://doi.org/10.1016/j.ejmech.2020.112652
21. M. Kumari, S. Tahlan, B. Narasimhan, K. Ramasamy, S.M. Lim, S.A.A. Shah, V. Mani and S. Kakkar, *BMC Chem*., **15**, 5 (2021); https://doi.org/10.1186/s13065-020-00717-y
22. S.A. Khan, M.J. Akhtar, U. Gogoi, D.U. Meenakshi and A. Das, *Pharmaceuticals*, **16**, 179 (2023); https://doi.org/10.3390/ph16020179
23. N. Naeem, E.U. Mughal, A. Sadiq, G.A. Othman and B. Shakoor, *Arch. Pharm*., **358**, e70059 (2025); https://doi.org/10.1002/ardp.70059
24. H.Y. Guo, Z.A. Chen, Q.K. Shen and Z.S. Quan, *J. Enzyme Inhib. Med. Chem*., **36**, 1115 (2021); https://doi.org/10.1080/14756366.2021.1890066
25. M.M. Matin, P. Matin, M.R. Rahman, T. Ben Hadda, F.A. Almalki, S. Mahmud, M.M. Ghoneim, M. Alruwaily and S. Alshehri, *Front. Mol. Biosci*., **9**, 864286 (2022); https://doi.org/10.3389/fmolb.2022.864286
26. V. Parthasarathi and H. Kanagaraj, *Curr. Top. Med. Chem*., **24**, 2033 (2024); https://doi.org/10.2174/0115680266308359240708094001
27. T. Azim, M. Wasim, M.S. Akhtar and I. Akram, *BMC Complement. Med. Ther*., **21**, 304 (2021); https://doi.org/10.1186/s12906-021-03485-x
28. M.M.S. Hamoud, N.A. Osman, S. Rezq, H.A.A. Abd El-Wahab, A.E.A. Hassan, H.A. Abdel-Fattah, D.G. Romero and A.M. Ghanim, *Bioorg. Chem.*, **124**, 105808 (2022); https://doi.org/10.1016/j.bioorg.2022.105808
29. W.A.A. Fadaly, M.T.M. Nemr, T.H. Zidan, F.E.A. Mohamed, M.M. Abdelhakeem, N.N. Abu Jayab, H.A. Omar and K.R.A. Abdellatif, *J. Enzyme Inhib. Med. Chem*., **38**, 2290461 (2023); https://doi.org/10.1080/14756366.2023.2290461
30. T. Glomb, J. Minta, M. Nowosadko, J. Radzikowska and P. Świątek, *Molecules*, **29**, 6036 (2024); https://doi.org/10.3390/molecules29246036
31. S. Pathania, R.K. Narang and R.K. Rawal, *Eur. J. Med. Chem*., **180**, 486 (2019); https://doi.org/10.1016/j.ejmech.2019.07.043
32. C. Zhao, K.P. Rakesh, L. Ravidar, W.Y. Fang and H.L. Qin, *Eur. J. Med. Chem*., **162**, 679 (2019); https://doi.org/10.1016/j.ejmech.2018.11.017
33. B. Kaur, G. Singh, V. Sharma and I. Singh, *Anticancer Agents Med. Chem*., **23**, 869 (2023); https://doi.org/10.2174/1871520623666221221143918
34. S. Shafi, M.M. Alam, N. Mulakayala, C. Mulakayala, G. Vanaja, A.M. Kalle, R. Pallu and M.S. Alam, *Eur. J. Med. Chem.*, **49**, 324 (2012); https://doi.org/10.1016/j.ejmech.2012.01.032
35. E.R. El-Sawy, A.B. Abdelwahab and G. Kirsch, *Molecules*, **27**, 2150 (2022); https://doi.org/10.3390/molecules27072150
36. P. Venkatesham, S.R. Parcha, S.L. Rath, R. Chedupaka and R.R. Vedula, *J. Heterocycl. Chem*., **60**, 1989 (2023); https://doi.org/10.1002/jhet.4728
37. R. Siddiqui, S. Shamim, S. Akhter, S. Kausar, S. Yousuf, A.A. Altaf, Z.S. Saeed Saify and F. Ameen, *Heliyon*, **10**, e35122 (2024); https://doi.org/10.1016/j.heliyon.2024.e35122
38. A. Sahoo, S.S. Swain, K. Pakeeraiah, S.K. Paidesetty and M. Panda, *Int. J. Biol. Macromol.*, **331**, 148263 (2025); https://doi.org/10.1016/j.ijbiomac.2025.148263
39. S.S. Swain, A. Sahoo, S.R. Singh, J. Sahoo and S.K. Paidesetty, *J. Biomol. Struct. Dyn*., **43**, 7336 (2025); https://doi.org/10.1080/07391102.2024.2326666

40. J. Mahyavanshi, M. Shukla and K. Parmar, *Int. J. Appl. Chem*., **13**, 99 (2017); https://doi.org/10.5138/09761055.2034
41. M.M. Khalaf, H.M. Abd El-Lateef, M. Gouda, T.M.A. Ibrahim, H. El-Shamy, A.A. Abdelhamid, S. Al-Ghamdi, A.A. Amer, M.M. Alam and M.A. Gad, *J. Indian Chem. Soc*., **101**, 101466 (2024); https://doi.org/10.1016/j.jics.2024.101466
42. M. Jonsson, J. Jestoi, A.V. Nathanail, U.M. Kokkonen, M. Anttila, P. Koivisto, P. Karhunen and K. Peltonen, *Food Chem. Toxicol*., **53**, 2732 (2013); https://doi.org/10.1016/j.fct.2012.11.023
43. V. Puri, A. Sharma, P. Kumar, K. Dua, K. Huanbutta, I. Singh and T. Sangnim, *Polymers*, **14**, 3836 (2022); https://doi.org/10.3390/polym14183836
44. A. Ganeshpurkar and G. Rai, *Indian J. Pharmacol*., **45**, 66 (2013); https://doi.org/10.4103/0253-7613.106438
45. S.K. Paliwal, B. Sati, S. Faujdar and S. Sharma, *J. Tradit. Complement. Med*., **7**, 532 (2016); https://doi.org/10.1016/j.jtcme.2016.08.005
46. S. Dharmadeva, L.S. Galgamuwa, C. Prasadinie and N. Kumarasinghe, *Ayu*, **39**, 239 (2018); https://doi.org/10.4103/ayu.AYU_27_18
47. G.G. Meshram, A. Kumar, W. Rizvi, C.D. Tripathi and R.A. Khan, *J. Tradit. Complement. Med.*, **6**, 172 (2015); https://doi.org/10.1016/j.jtcme.2014.11.038
48. B. Ghodge, A. Kshirsagar and V. Navghare, *Beni-Suef Univ. J. Basic Appl. Sci*., **9**, 30 (2020); https://doi.org/10.1186/s43088-020-00056-w
49. G. Clarke, K.N. Ting, C. Wiart and J. Fry, *Antioxidants*, **2**, 1 (2013); https://doi.org/10.3390/antiox2010001
50. P. Saraf, B. Bhardwaj, A. Verma, M.A. Siddiqui, H. Verma, P. Kumar, S. Srivastava, S. Krishnamurthy, S. Srikrishna and S.K. Shrivastava, *RSC Med. Chem*., **16**, 200 (2024); https://doi.org/10.1039/D4MD00471J
51. Y. Onodera, T. Teramura, T. Takehara, K. Shigi and K. Fukuda, *FEBS Open Bio*, **5**, 492 (2015); https://doi.org/10.1016/j.fob.2015.06.001
52. J. Chen, M. Si, Y. Wang, L. Liu, Y. Zhang, A. Zhou and W. Wei, *Inflammopharmacology*, **27**, 157 (2019); https://doi.org/10.1007/s10787-018-0504-y
53. M. Ahmadi, M. Bekeschus, K.D. Weltmann, K. von Woedtke and K. Wende, *RSC Med. Chem*., **13**, 471 (2022); https://doi.org/10.1039/D1MD00280E
54. S. Chahal, P. Rani, Kiran, J. Sindhu, G. Joshi, S. Kalyaanamoorthy, A. Ganesan, Mayank, P. Kumar, R. Singh and A. Negi, *ACS Omega*, **8**, 17446 (2023); https://doi.org/10.1021/acsomega.3c00692
55. A.E. Evren, A.Z. Kaya, A. Karakaya, B. Tutuş, E.M. Güngör, D. Nuha, D. Osmaniye, B. Kaya, U.A. Çevik, L. Yurttaş and Z.A. Kaplancikli, *Future Med. Chem*., **17**, 1899 (2025); https://doi.org/10.1080/17568919.2025.2546783
56. U.K. Purakkel, G. Praveena, E.W. Blanch and S. Maniam, *Chem. Rec*., e202500151 (2025); https://doi.org/10.1002/tcr.202500151